



Short communication

Identification of glutaredoxin 1 and glutaredoxin 2 genes from *Venerupis philippinarum* and their responses to benzo[a]pyrene and bacterial challenge

Changkao Mu^a, Qing Wang^{b,*}, Zeyi Yuan^c, Zhendong Zhang^d, Chunlin Wang^{a,**}

^a School of Marine Science of Ningbo University, Ningbo 315211, PR China

^b Key Laboratory of Coastal Zone Environmental Processes, CAS, Shandong Provincial Key Laboratory of Coastal Zone Environmental Processes, Yantai Institute of Coastal Zone Research, Chinese Academy of Sciences, 17 Chunhui Road, Yantai 264003, PR China

^c National Marine Data and Information Service, Tianjin 300171, PR China

^d National Marine Environmental Monitoring Center, Dalian 116023, PR China

ARTICLE INFO

Article history:

Received 9 October 2011

Received in revised form

5 December 2011

Accepted 5 December 2011

Available online 16 December 2011

Keywords:

Glutaredoxin

Venerupis philippinarum

Benzo[a]pyrene exposure

Bacterial challenge

ABSTRACT

Glutaredoxin (abbreviated as Grx) is an important ubiquitous disulfide reductase, which can protect organisms against oxidative stresses. In the present study, a monothiol glutaredoxin gene (named as VpGrx1) and a dithiol glutaredoxin gene (named as VpGrx2) were identified from *Venerupis philippinarum*. Similar to most Grx2s, VpGrx2 possessed the conserved catalytic residues (C–P–Y–C) and other conserved features critical for the fundamental structure and function of Grx2s, while the active motif (C–G–Y–S) of VpGrx1 was different from the counterpart in other Grx1s. Quantitative Real-time PCR assay showed that VpGrx1 and VpGrx2 transcripts were detected in a wide range of tissues and mainly distributed in gills and hepatopancreas. After *Vibrio* challenge, both the expression levels of VpGrx1 and VpGrx2 mRNA in hemocytes were significantly up-regulated at 24 h. As concerned to benzo[a]pyrene (BaP) exposure, the expression levels of VpGrx1 and VpGrx2 transcripts in hepatopancreas were also significantly induced at 24 h. These results suggested that ROS could be induced through the respiratory burst to clear the invading bacteria and pollutants. VpGrx1 and VpGrx2 perhaps involved in the regulation of redox homeostasis and innate immune responses of *V. philippinarum*.

© 2011 Elsevier Ltd. All rights reserved.

1. Introduction

Reactive oxygen species (ROS) including hydrogen peroxide, superoxide radical, hydroxyl radical and singlet oxygen, are natural products of oxidative metabolism in most aerobic organisms [1]. Small amounts of ROS are a cellular requirement because they are involved in signaling pathways and in regulation of a variety of cellular activities and gene expression [2]. However, excessive ROS production increases oxidative damage in the cell, possibly by altering or inactivating proteins, lipid membranes, and DNA [3]. Organisms have developed multilayered interdependent antioxidant system to defend against oxidative injury. Glutathione peroxidase, glutathione reductase, glutaredoxin, catalase and superoxide dismutase are the enzymes that participate in the dismutation of the ROS [4].

Glutaredoxins (Grxs) are small ubiquitous oxidoreductases that belong to the thioredoxin (Trx) superfamily and usually contain

a CxxC/S active-site motif [5]. Generally, Grxs can be categorized into three groups according to their structure and active site sequences [5]. The first group contains the classical Grxs of about 9–14 kDa with two cysteines in their active site, such as *Escherichia coli* Grx1 and the human Grxs [6]. The second group mainly consists of the monothiol Grxs like yeast Grx3, Grx4, and Grx5 [7]. The third type, represented by *E. coli* Grx2, corresponds to a very particular type of glutaredoxin presenting more homologies with glutathione S-transferase (GST) than with other Grxs [8]. With NADPH-dependent glutathione reductase (GR) and reduced glutathione (GSH) as reductants, Grxs are able to reduce disulfide bridges or glutathionylated proteins [9]. It has been well acknowledged that Grx/GSH/GR was one of the major redox systems involved in the maintenance of the thiol reduced state [10]. Grxs catalyze the GSH-dependent reduction of protein disulfides and GSH–protein mixed disulfides via two distinct mechanisms. The dithiol mechanism relies on two cysteine residues in the active site, whereas the monothiol mechanism only requires the extra N-terminal cysteine residue [9].

Grxs participate in many cellular processes, including protein folding and regulation, reduction of dehydroascorbate, protection

* Corresponding author. Tel.: +86 535 2109189; fax: +86 535 2109000.

** Corresponding author. Tel.: +86 057487600356; fax: +86 057487608374.

E-mail addresses: qingwang@yic.ac.cn (Q. Wang), wangchunlin@nbu.edu.cn (C. Wang).

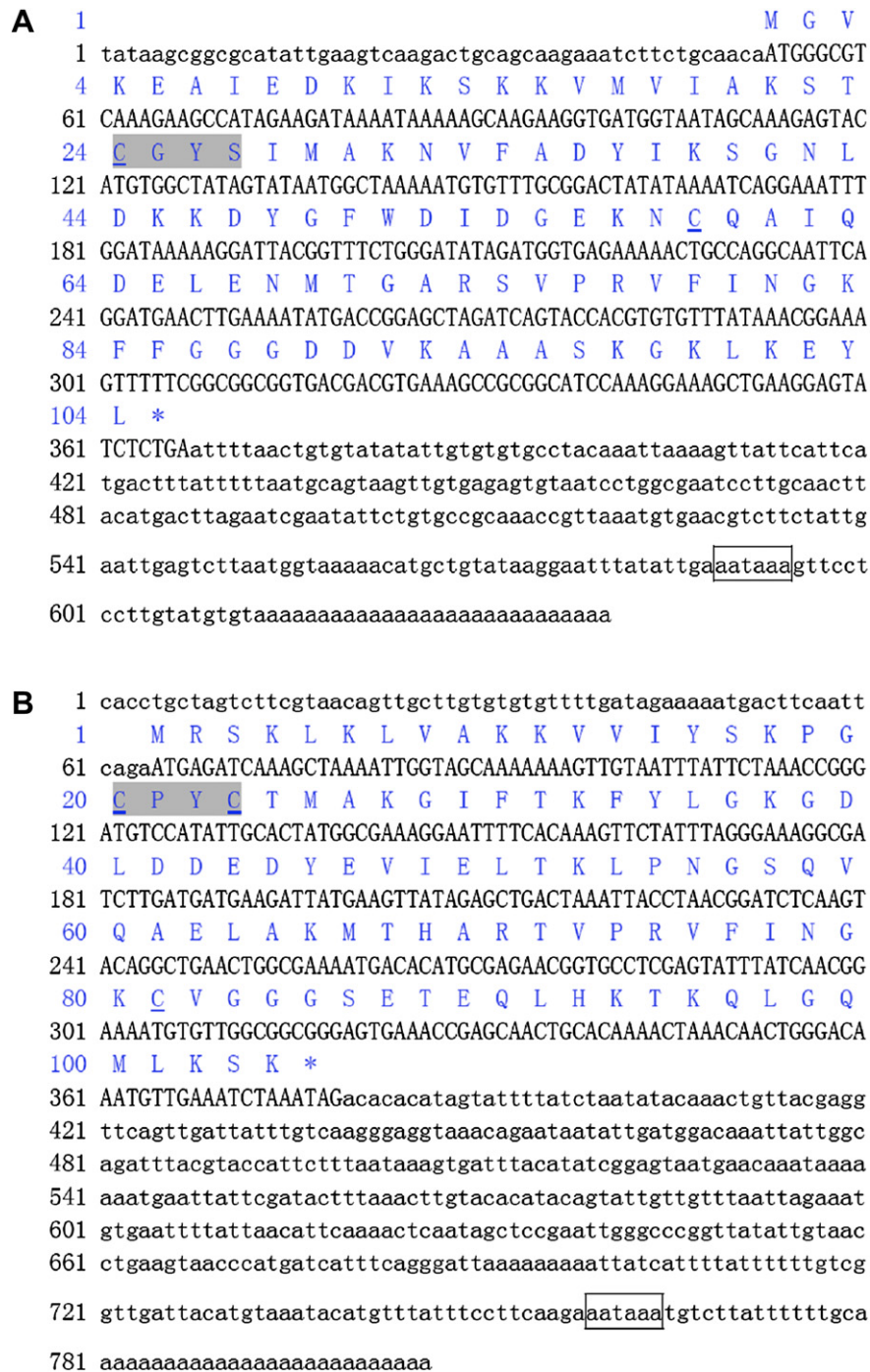


Fig. 1. Nucleotide and deduced amino acid sequences of VpGrx1 (A) and VpGrx2 (B). The asterisk (*) indicates the stop codon. Polyadenylation signal is included in a box. The active cysteine residues are underlined, and the catalytic center is shadowed. The other cysteine residue, Cys⁵⁹ in VpGrx1, and Cys⁸¹ in VpGrx2 are also underlined.

against reactive oxygen species, apoptosis and sulfur metabolism [6,11–14]. In addition, Grxs have the ability to reduce certain types of peroxiredoxins [15] and participate in the regulation of several transcription factors related to oxidative stress signaling in mammals [16]. To our knowledge, most studies about Grxs have been performed in *E. coli*, yeast, mammal cells and plants [6–8,17]. However, there are rare reports about Grxs and their functions in marine invertebrates so far.

The manila clam, *Venerupis philippinarum*, is an economically important sea food and widely cultured in China [18]. In recent years,

clam culture has suffered from massive mortality problem in China, which may be ascribed to bacterial infection and marine environmental pollutions [19]. Therefore, understanding the immune response of manila clam to bacterial challenge and pollutants exposure will facilitate the development of health care management in clam culture. In this study, the full-length cDNA of Grx1 and Grx2 were identified from *V. philippinarum*, and the expression profiles of VpGrx1 and VpGrx2 transcript under bacterial challenge and benzo [a]pyrene exposure were also investigated, hopefully laid the foundation for understanding the function of Grx in marine invertebrate.

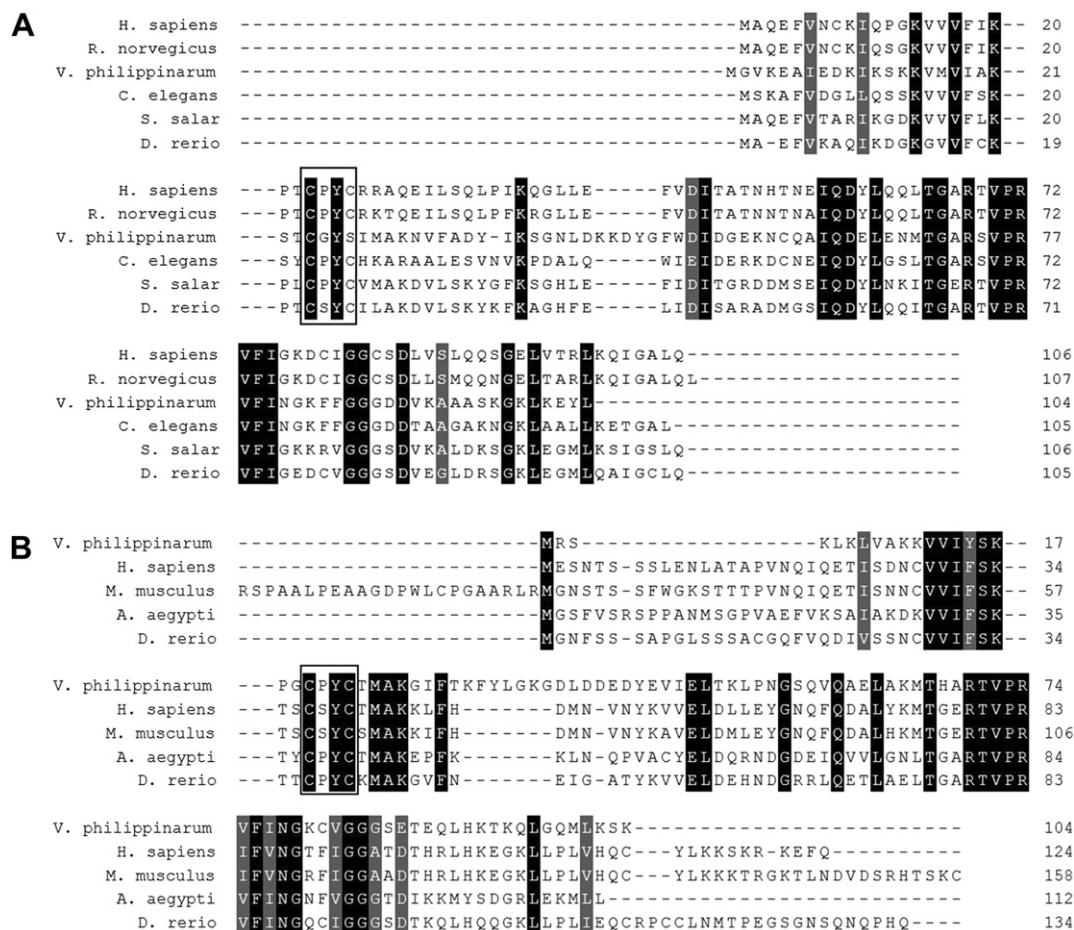


Fig. 2. Multiple alignment of VpGrx1 (A) and VpGrx2 (B) with corresponding counterparts deposited in GenBank. The black shadow region indicates positions where all sequences share the same amino acid residue. Gaps are indicated by dashes to improve the alignment. The species and the GenBank accession no. are as follows: NP_490812.1 (*Caenorhabditis elegans*), AC167872.1 (*Salmo salar*), NP_001005942.1 (*Danio rerio*), NP_071614.1 (*Rattus norvegicus*), BAA04769.1 (*Homo sapiens*), ABF18388.1 (*Aedes aegypti*), NP_001002404.1 (*Danio rerio*), AAH65387.1 (*Mus musculus*), and NP_001230328.1 (*Homo sapiens*).

2. Materials and methods

2.1. Animal culture and challenge

Adult clams *V. philippinarum* (shell-length: 3.0–4.0 cm) were collected from a local culturing farm and acclimatized in aerated seawater (33 psu) at 25 °C for 10 days before commencement of the experiment. During the acclimatization period, the clams were fed with *Isochrysis galbana* and *Platymonas helgolandica*, and the water was totally exchanged daily. After the acclimatization period, the clams were cultured in 20 L glass aquarium tanks, each containing 30 individuals.

For the bacterial challenge, *Vibrio anguillarum* was cultured at 28 °C in 2216E broth for 24 h, and then centrifuged to discard the broth. The clams were exposed to 10^7 CFU/mL vibrio as adjusted with filtered seawater. For the BaP exposure, the clams were treated with BaP at the concentration of 50 µg/L and 0.002% DMSO (v/v) respectively. The untreated clams were employed as the blank. The hemocytes and hepatopancreas of four clams were randomly sampled for gene expression analysis at 6, 12, 24, 48 and 96 h after bacterial exposure, and at 24, 48 and 96 h after BaP exposure respectively. Total mRNA was immediately extracted using Trizol reagent according to the manufacture's protocol (Invitrogen, USA).

2.2. Cloning the full-length cDNA of VpGrx1 and VpGrx2

BLAST analysis of all expressed sequence tags (ESTs) from a cDNA library of *V. philippinarum* revealed that two ESTs were highly similar to the previously identified Grx1s and Grx2s, respectively. The 5' and 3' ends of VpGrx1 and VpGrx2 were obtained by rapid amplification of cDNA ends (RACE) using the SMART RACE cDNA Amplification Kit (Clontech, USA). The PCR products were gel-purified and subcloned into pMD18-T simple vector (Takara). After being transformed into the competent cells of *E. coli* Top10F', three positive clones were sequenced on an ABI3730 Automated Sequencer (Applied Biosystem).

2.3. Sequence analysis of VpGrx1 and VpGrx2

The cDNA and amino acid sequences of VpGrx1 and VpGrx2 were analyzed using the BLAST algorithm at NCBI web site (<http://www.ncbi.nlm.nih.gov/blast>). Multiple alignments of VpGrx1 and VpGrx2 were performed with the ClustalW program (<http://www.ebi.ac.uk/clustalw/>). A phylogenetic tree was constructed with Mega4.1 software using the neighbor-joining (NJ) method and a Poisson correction model based on the alignment of amino acids [20]. Bootstrap analysis was used with 1000 replicates to test the relative support for the branches produced by the NJ analysis [21].

2.4. Tissue-specific expression of VpGrx1 and VpGrx2 mRNA

Hemocytes, gill, hepatopancreas, mantle and adductor muscle were taken aseptically from four clams and subjected to total RNA extraction. One microgram of total RNA was used for cDNA synthesis according to the manufacture's protocol (Promega, USA). qRT-PCR was carried out in an ABI 7500 Real-time Detection System by using the SYBR ExScript qRT-PCR Kit (Takara) as described previously [22]. The expression levels of VpGrx1 and VpGrx2 were analyzed using $2^{-\Delta\Delta CT}$ method [23] with β -actin mRNA as the control. The primers used to amplify the β -actin gene were P1 (5'-CTCCCTTGAGAAGAGCTACGA-3') and P2 (5'-GATAC-CAGCAGATTCCATACCC-3'). Two sets of gene-specific primers, P3 (5'-GGCGTCAAAGAAGCCATAGA-3') and P4 (5'-ATTGCCTGG-CAGTTTTTCTC-3') for VpGrx1, P5 (5'-GGCGAAAGGAATTTTCACAA-3') and P6 (5'-ATACTCGAGGCACCGTTCTC-3') for VpGrx2, were designed to amplify products of 182 bp and 152 bp, respectively. All data are given in terms of relative mRNA abundance, expressed as means plus or minus standard errors of the means (S.E.).

2.5. Temporal expression profile of VpGrx1 and VpGrx2 mRNA in hemocytes and hepatopancreas after bacterial challenge or BaP exposure

The tissues of hepatopancreas and hemocytes were selected to analyze temporal expression profile of VpGrx1 and VpGrx2 challenged by bacteria and BaP, respectively. The RNA extraction, cDNA synthesis, reaction component, thermal profile, and the data analysis were conducted as previously described [22].

2.6. Statistical analysis

SPSS 16.0 software (SPSS Inc., USA) was used for statistical analysis. All data were given in terms of relative mRNA expression as means \pm S.E. One-way analysis of variance (one-way ANOVA) was performed on all data and $P < 0.05$ was considered statistically significant.

3. Results and discussion

3.1. cDNA cloning and sequence analysis of VpGrx1 and VpGrx2

Two nucleotide sequences of 640 bp and 806 bp representing the complete cDNA sequence of VpGrx1 (Fig. 1A) and VpGrx2 (Fig. 1B) were obtained by overlapping EST and the amplified fragments. The sequences of VpGrx1 and VpGrx2 were deposited in GenBank under accession number GQ384390 and GQ384391 respectively. The deduced amino acid sequences of VpGrx1 and VpGrx2 were shown below their corresponding nucleotide sequences respectively in Fig. 1.

Both VpGrx1 and VpGrx2 encode a polypeptide of 104 amino acids, with a predicted molecular weight of 11.47 kDa and 11.55 kDa, and a theoretical pI of 8.81 and 9.52, respectively. The GSH binding sites of VpGrx1 are formed by Lys²¹, Cys²⁴, Tyr²⁶, Arg⁷³–Pro⁷⁶ and Gly⁸⁷–Asp⁹⁰. However, the GSH binding sites of VpGrx2 was formed by Lys¹⁷, Cys²⁰, Tyr²², Ala⁶⁹–Val⁷² and Gly⁸⁴–Glu⁸⁷. The GSH binding sites of VpGrx1 and VpGrx2 are found similar to that of human Grx2 [24].

3.2. Homology and phylogenetic analysis

Blastx analysis revealed that VpGrx1 shared significant homology with Grx1s from nematoda *Caenorhabditis elegans* (NP_490812.1, 46% identity), northern pike *Esox lucius* (AC013400.1, 47% identity), Atlantic salmon *Salmo salar* (ACI67872.1, 46% identity) and zebrafish *Danio rerio* (NP_001005942.1, 40% identity), while VpGrx2 displayed high similarity with Grx2s from zebrafish *D. rerio* (NP_001002404.1, 51% identity), abalone *Haliotis diversicolor supertexta* (ABW04624.1, 43% identity), western clawed frog *Xenopus (Silurana) tropicalis* (NP_001016637.1, 43% identity) and human *Homo sapiens* (AAH28113.1, 46% identity). According to the phylogenetic tree (Fig. 3), Grx1s and Grx2s were separated into two distinct groups (Grx4 as out-group). The Grx1s members were mainly clustered into two branches by their vertebrate and invertebrate origin. VpGrx1 was firstly formed a sister group with Grx1s from nematoda, and then grouped with those from urochordata

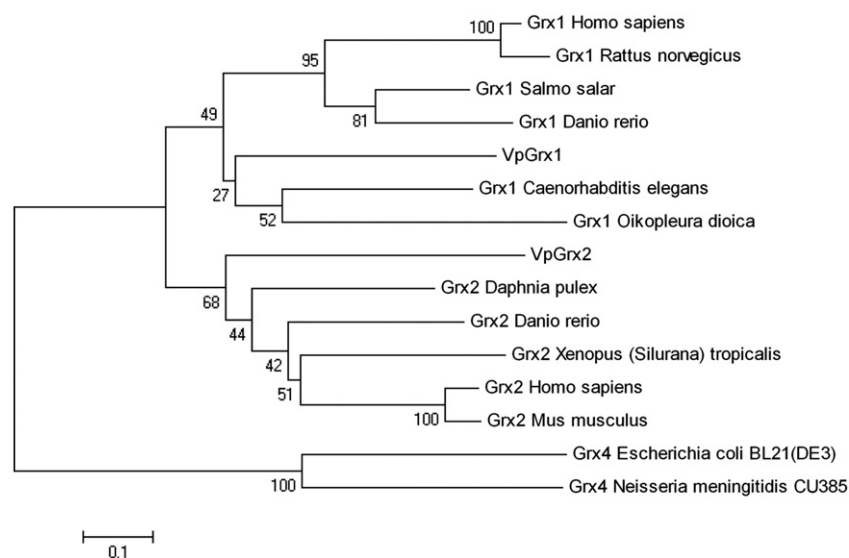


Fig. 3. Phylogenetic tree constructed by neighbor-joining method based on the sequences of Grx1 and Grx2 from different animals. The numbers at the forks indicate the bootstrap values (in %) out of 1000 replicates. The sequences were retrieved from the GenBank as follows: CBY11852.1 (*Oikopleura dioica*), NP_490812.1 (*Caenorhabditis elegans*), ACI67872.1 (*Salmo salar*), NP_001005942.1 (*Danio rerio*), NP_071614.1 (*Rattus norvegicus*), BAA04769.1 (*Homo sapiens*), EFX80727.1 (*Daphnia pulex*), NP_001016637.1 (*Xenopus (Silurana) tropicalis*), AAH65387.1 (*Mus musculus*), and NP_001230328.1 (*Homo sapiens*). The Grx4 sequences from *Neisseria meningitidis* CU385 (EGC62602.1) and *Escherichia coli* BL21(DE3) (CAQ32131.1) were used as out-group.

and further grouped with those from vertebrate. VpGrx2 formed a group with Grx2 from arthropod, and further grouped with the vertebrate Grx2s. The relationships displayed in the phylogenetic tree were in good agreement with traditional taxonomy.

Multiple alignments revealed that VpGrx1 and VpGrx2 both possessed the conserved features critical for the fundamental structure and function of the Grx proteins. The C–P/S–Y–C motif was highly conserved in all analyzed Grx1s and Grx2s with the exception of C–G–Y–S in VpGrx1 (Fig. 2). The monothiol active motif in VpGrx1 was different from typical Grx1s, suggesting VpGrx1 might catalyze the GSH-dependent reduction of GSH–protein mixed disulfides via the monothiol mechanism [10]. Similar phenomenon was also observed in a hypothetical Grx1 from *Oikopleura dioica* with an active motif of C–P–Y–S. These monothiol Grx1s had similar active motifs like those of the yeast Grx3, Grx4, and Grx5, but the length of monothiol Grx1s were shorter than those of the yeast Grx3, Grx4, and Grx5 [7]. VpGrx2 possessed the conserved motif C–P–Y–C and shared high identity with counterparts from arthropod and mammals. These characterizations suggested that VpGrx1 and VpGrx2 were new members of the Grx1 and Grx2 family, respectively.

3.3. Tissue-specific expression of VpGrx1 and VpGrx2

The tissue distributions of VpGrx1 and VpGrx2 mRNA were investigated by quantitative real-time PCR with β -actin as internal

control. For VpGrx1, VpGrx2 and β -actin genes, only one peak at the corresponding melting temperature was detected in the dissociation curve analysis, indicating that the PCR product was specifically amplified (data not shown). The mRNA transcripts of VpGrx1 and VpGrx2 were detected in all the examined tissues, including hepatopancreas, hemocytes, adductor muscle, mantle and gills, indicating a general role in physiological processes in various tissues. The VpGrx1 transcript was dominantly expressed in the tissue of gill and hepatopancreas, and moderately detected in hemocytes and mantle (Fig. 4A). A similar tissue-specific expression pattern was also observed for VpGrx2 transcript with the highest expression level in gill and lowest expression levels in adductor muscle (Fig. 4B).

The enrichment of VpGrx1 and VpGrx2 mRNA in gills and hepatopancreas suggested that these organs were the major sites for biotic and abiotic substances uptake and elimination and possessed a large amount of detoxifying enzymes in marine invertebrates [25].

3.4. Temporal expression profile of VpGrx1 and VpGrx2 mRNA in hemocytes after bacterial challenge

The temporal expression profiles of VpGrx1 and VpGrx2 transcripts after *Vibrio* challenge were shown in Fig. 5A and B, respectively. In the present study, DMSO (0.002%, v/v) posed no influence

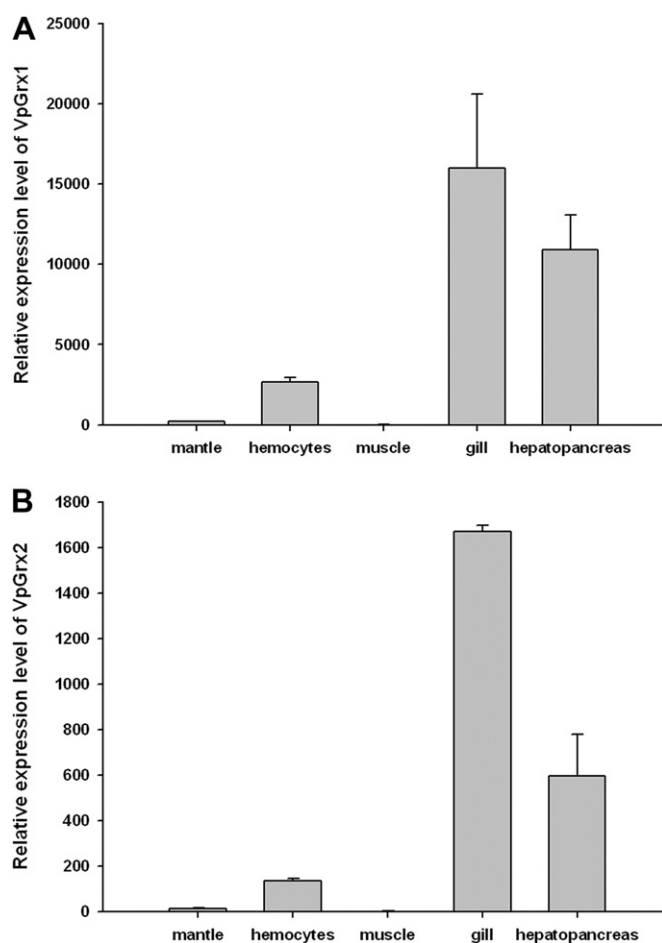


Fig. 4. VpGrx1 (A) and VpGrx2 (B) mRNA expression level in different tissues of adult clams detected by Real-time PCR. The transcript level VpGrx1 and VpGrx2 in hemocytes, gills, mantles, and hepatopancreas is normalized to that of adductor muscles, respectively. The results are shown as mean \pm S.E. ($n = 4$). Significance across control is indicated with an asterisk at $P < 0.05$.

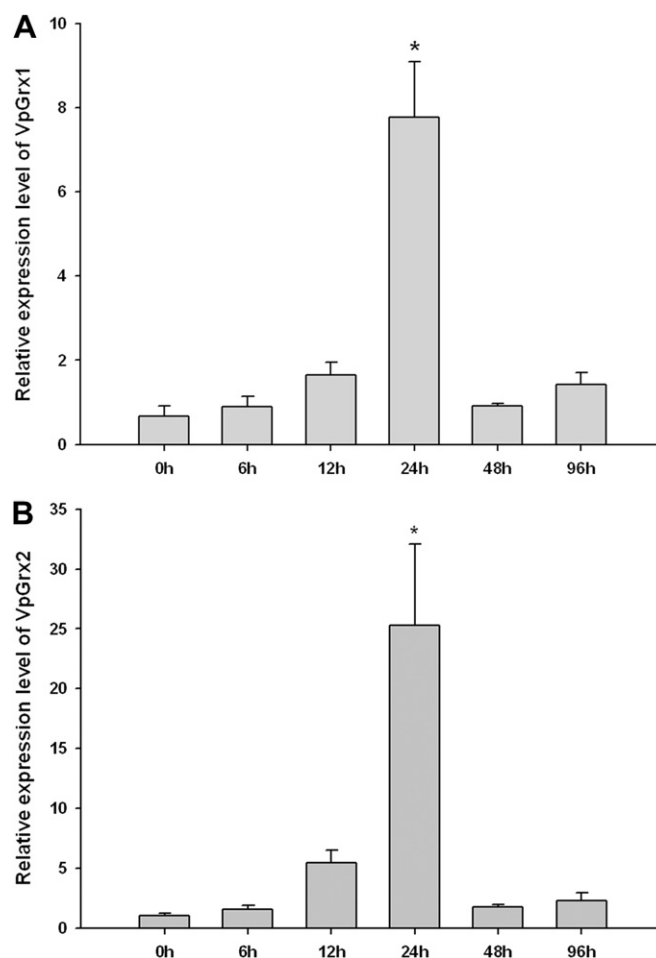


Fig. 5. Temporal expression profile of VpGrx1 (A) and VpGrx2 (B) mRNA in hemocytes after bacterial challenge measured by quantitative real-time PCR. The mRNA expression level is calculated relative to actin expression and shown as mean \pm S.E. ($n = 4$). Significance across control is indicated with an asterisk at $P < 0.05$.

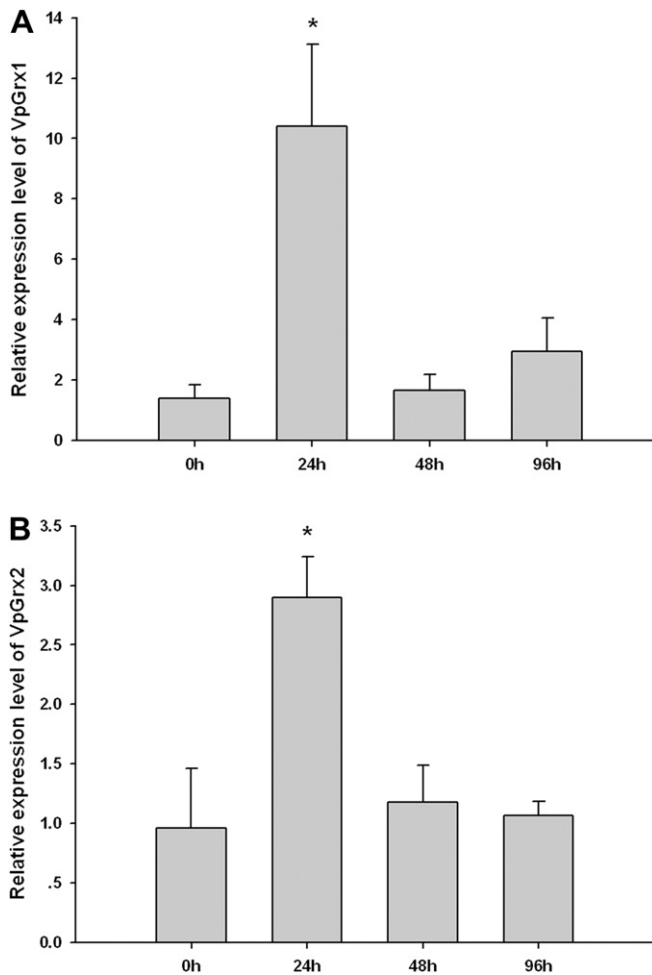


Fig. 6. Temporal expression profile of VpGrx1 (A) and VpGrx2 (B) mRNA in hepatopancreas after BaP (50 µg/L) exposure measured by quantitative real-time PCR. The mRNA expression level is calculated relative to actin expression and shown as mean \pm S.E. ($n = 4$). Significance across control is indicated with an asterisk at $P < 0.05$.

on the expression levels of VpGrx1 and VpGrx2 (data not shown). After bacterial challenge, the mRNA transcripts of both VpGrx1 and VpGrx2 increased slowly from 6 h to 12 h. Then, the expression levels of VpGrx1 and VpGrx2 were sharply up-regulated to 7.78-fold and 25.28-fold of the control group at 24 h respectively. After that, the expression levels of VpGrx1 and VpGrx2 recovered to the original level gradually. Statistical analysis revealed that significant difference of the expression levels of VpGrx1 and VpGrx2 was only observed at 24 h ($P < 0.01$) after bacterial exposure as compared to the control groups. It has been demonstrated that ROS could be induced through the respiratory burst to clear the invading microorganism [27]. However, the homeostasis of redox balance in cells would be disrupted because of ROS generation. Therefore, the change of Grx transcripts after bacterial challenge may be a mechanism to maintain the balance of redox state. In the present study, the higher expression level of VpGrx2 than that of VpGrx1 indicated that VpGrx2 may respond more sensitively to the oxidative stress induced by bacterial challenge.

3.5. Temporal expression profile of VpGrx1 and VpGrx2 mRNA in hepatopancreas after BaP exposure

The temporal expression profiles of VpGrx1 and VpGrx2 transcript after BaP stress were shown in Fig. 6A and B, respectively.

Both the expression levels of VpGrx1 and VpGrx2 were up-regulated to 10.41-fold and 2.90-fold of the control group at 24 h respectively. Then, the expression levels of VpGrx1 and VpGrx2 decreased back to the original level at 48 h and 96 h. Statistical analysis revealed that the expression levels of VpGrx1 and VpGrx2 were significantly higher than those of the control groups only at 24 h ($P < 0.01$).

In the present study, the expression levels of VpGrx1 and VpGrx2 in hepatopancreas were up-regulated after exposure to BaP, which indicated that both the transcripts of VpGrx1 and VpGrx2 responded sensitively to BaP stress. This may be explained by the fact that ROS increased quickly after the BaP stress [28] and a rapid activation of VpGrx1 and VpGrx2 mRNA transcription was required to ensure the synthesis of Grxs. As time progressed on, the ROS induced by BaP stress was eliminated by antioxidants including VpGrx1 and VpGrx2, and then the transcripts decreased to the original level at 96 h. It has been reported the expression of Grx transcript could be induced by pollutant exposure. For example, the expression of Grx C4 and Grx S12 in germinating pea *Pisum sativum* seeds was significantly increased under Cd stress conditions [17]. In the fungal *Glomus intraradices*, the Grx1 transcript level was also up-regulated under copper stress [29]. Thus, the Grxs have been suggested to play important roles in protecting these organisms from oxidative damage induced by pollutant exposure.

In conclusion, the full-length cDNAs encoding Grx1 and Grx2 were identified from *V. philippinarum*. VpGrx1 and VpGrx2 mRNA were constitutively expressed in the tested tissues, and both transcripts were up-regulated at 24 h after BaP and bacterial challenge. These results suggested that VpGrx1 and VpGrx2 perhaps played an essential role in maintenance of homeostasis and immune defense in *V. philippinarum*.

Acknowledgments

The authors were grateful to all the laboratory members for continuous technical advice and helpful discussion. This research was supported by National Key Technology Support Program (2011BAD13B00) and the K.C. Wong Magna Fund.

References

- [1] Nordberg J, Arner ES. Reactive oxygen species, antioxidants, and the mammalian thioredoxin system. *Free Radic Biol Med* 2001;31:1287–312.
- [2] D'Autreaux B, Toledano MB. ROS as signalling molecules: mechanisms that generate specificity in ROS homeostasis. *Nat Rev Mol Cell Biol* 2007;8:813–24.
- [3] Hensley K, Robinson KA, Gabbita SP, Salsman S, Floyd RA. Reactive oxygen-species, cell signaling, and cell injury. *Free Radic Biol Med* 2000;28:1456–62.
- [4] Rudneva I. Antioxidant system of Black Sea animals in early development. *Comp Biochem Physiol C* 1999;122:265–71.
- [5] Vlamis-Gardikas A, Holmgren A. Thioredoxin and glutaredoxin isoforms. *Methods Enzymol* 2002;347:286–96.
- [6] Lillig CH, Berndt C, Vergnolle O, Lonn ME, Hudemann C, Bill E, et al. Characterization of human glutaredoxin 2 as iron-sulfur protein: a possible role as redox sensor. *Proc Natl Acad Sci USA* 2005;102:8168–73.
- [7] Rodriguez-Manzanique MT, Ros J, Cabiscol E, Sorribas A, Herrero E. Grx5 glutaredoxin plays a central role in protection against protein oxidative damage in *Saccharomyces cerevisiae*. *Mol Cell Biol* 1999;19:8180–90.
- [8] Vlamis-Gardikas A, Aslund F, Spyrou G, Bergman T, Holmgren A. Cloning, overexpression, and characterization of glutaredoxin 2, an atypical glutaredoxin from *Escherichia coli*. *J Biol Chem* 1997;272:11236–43.
- [9] Fernandes AP, Holmgren A. Glutaredoxins: glutathione-dependent redox enzymes with functions far beyond a simple thioredoxin backup system. *Antioxid Redox Signal* 2004;6(1):63–74.
- [10] Rouhier N, Couturier J, Johnson MK, Jacquot JP. Glutaredoxins: roles in iron homeostasis. *Trends Biochem Sci* 2010;35:43–52.
- [11] Holmgren A. Thioredoxin and glutaredoxin systems. *J Biol Chem* 1989;264(24):13963–6.
- [12] Park JB, Levine M. Purification, cloning and expression of dehydroascorbic acid-reducing activity from human neutrophils: identification as glutaredoxin. *Biochem J* 1996;315:931–8.
- [13] Grant CM. Role of the glutathione/glutaredoxin and thioredoxin systems in yeast growth and response to stress conditions. *Mol Microbiol* 2001;39:533–41.

- [14] Chrestensen CA, Starke DW, Mieyal JJ. Acute cadmium exposure inactivates thioredoxin (glutaredoxin), inhibits intracellular reduction of protein-glutathionyl-mixed disulfides, and initiates apoptosis. *J Biol Chem* 2000;275:26556–65.
- [15] Rouhier N, Gelhaye E, Jacquot JP. Glutaredoxin dependent peroxiredoxin from poplar: protein–protein interaction and catalytic mechanism. *J Biol Chem* 2002;277:13609–14.
- [16] Rouhier N, Gelhaye E, Jacquot JP. Redox control by dithiol-disulfide exchange in plants: II. The cytosolic and mitochondrial systems. *Ann N Y Acad Sci* 2002; 973:520–8.
- [17] Smiri M, Chaoui A, Rouhier N, Gelhaye E, Jacquot JP, El Ferjani E. Cadmium affects the glutathione/glutaredoxin system in germinating pea seeds. *Biol Trace Elem Res* 2011;142:93–105.
- [18] Yan X, Zhang G, Yang F. Effects of diet, stocking density, and environmental factors on growth, survival, and metamorphosis of manila clam *Ruditapes philippinarum* larvae. *Aquaculture* 2006;253:350–8.
- [19] Zhang G, Li X, Xue Z. Potential reasons and controlling strategies of mollusk dramatic death in China. *Chin Fishery* 1999;9:34–9.
- [20] Kumar S, Dudley J, Nei M, Tamura K. MEGA: a biologist-centric software for evolutionary analysis of DNA and protein sequences. *Brief Bioinform* 2008;9: 299–306.
- [21] Felsenstein J. Confidence limits on phylogenies: an approach using bootstrap. *Evolution* 1985;39:783–91.
- [22] Wang Q, Ning X, Chen L, Pei D, Zhao J, Zhang L, et al. Responses of thioredoxin 1 and thioredoxin-related protein 14 mRNAs to cadmium and copper stresses in *Venerupis philippinarum*. *Comp Biochem Physiol C* 2011; 154:154–60.
- [23] Livak KJ, Schmittgen TD. Analysis of relative gene expression data using real-time quantitative PCR and the 2^{(-Delta Delta C(T))} method. *Methods* 2001;25: 402–8.
- [24] Lundberg M, Johansson C, Chandra J, Enoksson M, Jacobsson G, Ljung J, et al. Cloning and expression of anovel human glutaredoxin (Grx2) with mitochondrial and nuclear isoforms. *J Biol Chem* 2001;276:26269–75.
- [25] Livingstone DR. Organic xenobiotic metabolism in marine invertebrates. In: Gilles R, editor. *Adv Comp Environ Physiol*. 7th ed. Berlin: Springer; 1991. p. 45–185.
- [27] Segal A. How neutrophils kill microbes. *Annu Rev Immunol* 2005;23: 197–223.
- [28] Gomez-Mendikute A, Etxeberria A, Olabarrieta I, Cajaraville MP. Oxygen radicals production and actin filament disruption in bivalve haemocytes treated with benzo(a)pyrene. *Mar Environ Res* 2002;54:431–6.
- [29] Benabdellah K, Merlos MA, Azcon-Aguilar C, Ferrol N. GintGRX1, the first characterized glomeromycotan glutaredoxin, is a multifunctional enzyme that responds to oxidative stress. *Fungal Genet Biol* 2009;46: 94–103.